

**Gapless points of dimerized quantum spin chains: Analytical and numerical studies**

V. Ravi Chandra, Diptiman Sen, and Naveen Surendran

*Centre for High Energy Physics, Indian Institute of Science, Bangalore 560012, India*

(Received 22 August 2006; revised manuscript received 9 October 2006; published 21 November 2006)

We study the locations of the gapless points which occur for quantum spin chains of finite length (with a twisted boundary condition) at particular values of the nearest-neighbor dimerization, as a function of the spin  $S$  and the number of sites. For strong dimerization and large values of  $S$ , a tunneling calculation reproduces the same results as those obtained from more involved field theoretic methods using the nonlinear  $\sigma$ -model approach. A different analytical calculation of the matrix element between the two Néel states gives a set of gapless points; for strong dimerization, these differ significantly from the tunneling values. Finally, the exact diagonalization method for a finite number of sites yields a set of gapless points which are in good agreement with the Néel state calculations for all values of the dimerization, but the agreement with the tunneling values is not very good even for large  $S$ . This raises questions about possible corrections to the tunneling results.

DOI: [10.1103/PhysRevB.74.184424](https://doi.org/10.1103/PhysRevB.74.184424)

PACS number(s): 75.10.Jm, 75.10.Pq, 73.43.Nq

**I. INTRODUCTION**

One-dimensional quantum spin systems have been studied extensively for many years, particularly after Haldane predicted theoretically that Heisenberg integer spin chains should have a gap between the ground state and the first excited state,<sup>1</sup> and this was then observed experimentally in a spin-1 system.<sup>2</sup> Haldane's analysis used a nonlinear  $\sigma$ -model (NLSM) which is a field theoretic description of the long-distance and low-energy modes of the spin system.<sup>3-7</sup>

Although the NLSM approach is supposed to be accurate only for large values of the spin  $S$ , it is found to be qualitatively correct even for small values of  $S$ . For instance, if there is a dimerization in the nearest-neighbor Heisenberg couplings, taken to be 1 and  $\kappa$  alternately, the NLSM predicts that there is a discrete set of values of  $\kappa$  lying in the range  $0 \leq \kappa \leq 1$  for which the spin chain is gapless; these correspond to quantum phase transitions. Further, the number of gapless points is predicted to be the number of integers  $\leq S + 1/2$ ; in particular, the undimerized chain (with  $\kappa = 1$ ) is a gapless point if  $S$  is a half-odd-integer. Numerical analysis shows this to be true for values of  $S$  up to 2;<sup>8-13</sup> however, the numerically obtained values of  $\kappa$  at the gapless points do not agree well with the NLSM values. It therefore appears that there must be corrections to the NLSM analysis for small values of  $S$ .

The NLSM approach that has been used so far to find the gapless points is based on certain properties of a field theory in two dimensions (one space and one time); the gapless points occur when the coefficient of a topological term is given by  $\pi$  modulo  $2\pi$  (as will be discussed in Sec. II). Although there are arguments justifying this criterion,<sup>14</sup> there does not seem to be a simple physical picture behind it. One of the aims of our paper will be to provide a picture based on tunneling between two classical ground states.

Numerically, there are different ways of finding the gapless points for a dimerized spin chain. One of the most accurate ways is based on exact diagonalization studies of a finite spin chain with a twisted boundary condition, to be specified more precisely in Sec. II.<sup>12,15</sup> In the presence of the twist, it is found that the gap between the ground state and first excited state vanishes at a value of  $\kappa$  which is a function of the number of sites  $2N$  (we use this notation since the

number of sites will always be taken to be even). We will be mainly interested in finite system sizes in our work; however, it is known from conformal field theory<sup>12,15-18</sup> that the locations of gapless points for the infinite system can be found very accurately by finding the locations of those points for finite systems, and then extrapolating to  $N \rightarrow \infty$ .

In this paper, we will use three different approaches to study finite systems with a twisted boundary condition, in order to find the gapless points as a function of  $S$  and  $N$ . The first two approaches will be analytical; they will be based on the idea that in the presence of a twist, the system has two classical ground states, called Néel states, which are degenerate. The degeneracy may be broken in quantum mechanics by tunneling. However, if the tunneling amplitude is zero, we get a gapless point in the sense that the lowest two states have the same energy. The third approach will be numerical and will be based on exact diagonalization of finite systems using various symmetries.

In Sec. II, we will first define the dimerized quantum spin chain and review how it can be described using a NLSM field theory. We will then describe the twisted boundary condition for a finite system. In Sec. III, we will describe our first analytical approach. This is based on a tunneling calculation for a chain with a finite number of sites. For reasons explained below, this method is limited to small values of  $\kappa$ . We will see that the expressions for the scale of the gap and the locations of the gapless points agree with those obtained from the NLSM field theory; this is remarkable because our analysis will be based only on quantum mechanical tunneling in a finite system, while the field theoretic analysis is based on a renormalization group equation and the presence of a topological term. Our second approach, described in Sec. IV, is based on a direct quantum mechanical calculation of the matrix element between the two Néel states to lowest order in the Hamiltonian; this method works for all values of  $\kappa$ . We will see that the locations of the gapless points obtained by the two methods differ substantially for small  $\kappa$ . We make some speculations about how the tunneling results may be corrected. In Sec. V, we use exact diagonalization to find the gaps and the locations of the gapless points as functions of  $\kappa$  for different values of  $S$  and  $N$ . We find that the numerical results for the locations of the gapless points agree quite well with those found by the second analytical method,

and therefore disagree with those found by the tunneling approach. In Sec. VI, we will summarize our results.

## II. DIMERIZED QUANTUM SPIN CHAIN

### A. Field theoretic description

In this section, we will briefly review the NLSM field theory for a dimerized spin chain with an infinite number of sites. The Hamiltonian is given by

$$H = \sum_i [\vec{S}_{2i-1} \cdot \vec{S}_{2i} + \kappa \vec{S}_{2i} \cdot \vec{S}_{2i+1}], \quad (1)$$

where we have spin  $S$  at every site, and  $\kappa \geq 0$ . This describes a Heisenberg antiferromagnetic spin chain since all the couplings are positive. We will set  $\hbar = 1$ , so that  $\vec{S}_i^2 = S(S+1)$ . We will specify the appropriate boundary conditions when we discuss finite systems below. In many papers, the nearest-neighbor couplings are taken to be  $1 + \delta$  and  $1 - \delta$ , instead of  $1$  and  $\kappa$ . After a rescaling of the Hamiltonian, we see that the two parameters are related as

$$\kappa = \frac{1 - \delta}{1 + \delta}. \quad (2)$$

In the classical limit  $S \rightarrow \infty$ , the ground state of Eq. (1) is given by a configuration in which all the spins at odd sites point in the same direction while all the spins at even sites point in the opposite direction. This motivates us to define a variable

$$\vec{\phi}(x) = \frac{\vec{S}_{2n-1} - \vec{S}_{2n}}{2S}, \quad (3)$$

where  $x = 2na$  denotes the spatial coordinate and  $a$  is the lattice spacing;  $x$  becomes a continuous variable in the limit  $a \rightarrow 0$ . In the classical limit,  $\vec{\phi}$  becomes a unit vector in three dimensions; the model is called the NLSM because of this nonlinear constraint. One can then derive an action in terms of the field  $\vec{\phi}(x, t)$ ; this takes the form<sup>1,3</sup>

$$\begin{aligned} S = \int dt dx & \left[ \frac{1}{2cg} \left( \frac{\partial \vec{\phi}}{\partial t} \right)^2 - \frac{c}{2g} \left( \frac{\partial \vec{\phi}}{\partial x} \right)^2 \right] \\ & + \frac{\theta}{4\pi} \int dt dx \vec{\phi} \cdot \frac{\partial \vec{\phi}}{\partial t} \times \frac{\partial \vec{\phi}}{\partial x}, \end{aligned} \quad (4)$$

where

$$\begin{aligned} c &= 2aS\sqrt{\kappa}, \\ g &= \frac{1}{S} \frac{1 + \kappa}{\sqrt{\kappa}}, \\ \theta &= 4\pi S \frac{\kappa}{1 + \kappa}. \end{aligned} \quad (5)$$

The parameters  $c$ ,  $g$ , and  $\theta$  denote the spin wave velocity, the strength of the interactions between the spin waves, and the

coefficient of a topological term, respectively. One can show that the term multiplying  $\theta$  in Eq. (4) is topological in the sense that its value is always an integer. Even though the first two terms in Eq. (4) are quadratic, it describes an interacting theory because of the nonlinear constraint on  $\vec{\phi}$ .

It is known that the system governed by Eq. (4) is gapless if  $\theta = \pi$  modulo  $2\pi$  and  $g$  is less than a critical value.<sup>1,3,14</sup> This implies that the theory is gapless if  $4S\kappa/(1+\kappa) = 1, 3, \dots$  and  $g$  is small enough. In particular, this means that in the range  $0 \leq \kappa \leq 1$ , there are a discrete set of values of  $\kappa$  for which the system is gapless; the number of such values is given by the number of integers  $\leq S + 1/2$ . For all values of  $\theta \neq \pi$  modulo  $2\pi$ , the system is gapped. For  $\theta = 0$  modulo  $2\pi$ , the gap is given by  $\exp(-2\pi/g)$ . This follows from the fact that the interaction  $g$  effectively becomes a function of the length scale  $L$  and satisfies a renormalization group equation of the form  $dg_{eff}/d \ln L = g_{eff}^2/(2\pi)$ . This implies that  $g_{eff}(L)$  becomes very large at a length scale given by  $L_0 \sim a \exp(2\pi/g)$ , where  $g = g_{eff}(a)$  is given in Eq. (5). This is the correlation length of the system; the energy gap is related to the inverse of this length, namely,  $\Delta E \sim c \exp(-2\pi/g)$ .

### B. Twisted boundary condition

In this section, we will study the same model as in Eq. (1) but with a finite number of sites going from 1 to  $2N$ . Although a periodic boundary condition would appear to be the simplest, it turns out that a more useful boundary condition is one with a twist.<sup>12,15,19</sup> We define the Hamiltonian to be

$$\begin{aligned} H = \sum_{n=1}^N & [S_{2n-1}^x S_{2n}^x + S_{2n-1}^y S_{2n}^y + S_{2n-1}^z S_{2n}^z] + \kappa \sum_{n=1}^{N-1} [S_{2n}^x S_{2n+1}^x \\ & + S_{2n}^y S_{2n+1}^y + S_{2n}^z S_{2n+1}^z] + \kappa [-S_{2N}^x S_1^x - S_{2N}^y S_1^y + S_{2N}^z S_1^z]. \end{aligned} \quad (6)$$

Note that the bond going from site  $2N$  to site 1, to be called the bond  $(2N, 1)$  for short, has a minus sign for the  $xx$  and  $yy$  couplings. We will call this a twisted boundary condition; it is equivalent to rotating the  $x$  and  $y$  components of  $\vec{S}_1$  by  $\pi$  about the  $z$  axis just for that bond.

An advantage of the twisted boundary condition is that classically, the Hamiltonian in Eq. (6) has exactly two ground states, namely, (i)  $\vec{S}_{2n-1} = (0, 0, S)$  and  $\vec{S}_{2n} = (0, 0, -S)$  for all  $n$ , and (ii)  $\vec{S}_{2n-1} = (0, 0, -S)$  and  $\vec{S}_{2n} = (0, 0, S)$  for all  $n$ . We will call these two Néel states  $N_1$  and  $N_2$ , respectively. (This is in contrast to the case of periodic boundary conditions where there is an infinite family of classical ground states because  $\vec{S}_{2n-1} = -\vec{S}_{2n}$  can point in any direction.) If the classical degeneracy is broken quantum mechanically in any way, there will be a gap between the lowest two states of the system, while if the degeneracy remains unbroken, the system will be gapless. In Secs. III and IV, we will describe two ways of analytically studying whether the degeneracy is broken.

Let us now describe the various symmetries of the Hamiltonian in Eq. (6). Although the total spin is not a good

quantum number because of the twist on one bond,  $S_{tot}^z = \sum_n (S_{2n-1}^z + S_{2n}^z)$  is a good quantum number.

Equation (6) satisfies the duality property  $H(\kappa) = \kappa \tilde{H}(1/\kappa)$ , where  $\tilde{H}$  is related to  $H$  by a unitary transformation. The unitary transformation is required because the twist only exists at the bond  $(2N, 1)$  whose strength is  $\kappa$ . By applying a rotation  $S_1^x \rightarrow -S_1^x$  and  $S_1^y \rightarrow -S_1^y$ , we can move the twist from the bond  $(2N, 1)$  to the bond  $(1, 2)$ . Since a unitary transformation does not affect the spectrum, we conclude that if there is a gapless point at a value  $\kappa$ , there must also be a gapless point at  $1/\kappa$ .

Next, we define the parity transformation  $P$  as reflection of the system about the bond  $(2N, 1)$ , namely,

$$\vec{S}_i \leftrightarrow \vec{S}_{2N+1-i}. \quad (7)$$

This is a discrete symmetry of the Hamiltonian  $H$ , and all eigenstates of  $H$  will be eigenstates of  $P$  with eigenvalue  $\pm 1$ . For any value of  $\kappa$ , we find that the ground and first excited states always have opposite values of the parity. We will show below that the relative parity of the ground states in the limits  $\kappa \rightarrow 0$  and  $\kappa \rightarrow \infty$  is given by  $(-1)^{2S}$ . For integer  $S$ , this will imply that in the range  $0 < \kappa < \infty$ , the number of crossings between the ground state and the first excited state (and hence the number of gapless points) must be even. But for half-odd-integer  $S$ , the number of such crossings must be odd; combined with the duality  $\kappa \rightarrow 1/\kappa$ , this implies that there must be a crossing and therefore a gapless point at  $\kappa=1$  (this is a self-dual point).

To prove the statement about the relative parities of the ground states at  $\kappa \rightarrow 0$  and  $\kappa \rightarrow \infty$  being given by  $(-1)^{2S}$ , we proceed as follows. We first observe that if there are only two spins 1 and 2 governed by the untwisted Hamiltonian  $h_u = S_1^x S_2^x + S_1^y S_2^y + S_1^z S_2^z$ , then under the reflection  $1 \leftrightarrow 2$ , the ground state has the parity  $(-1)^{2S}$ , while the first excited state has the parity  $(-1)^{2S+1}$ ; but for the twisted Hamiltonian  $h_t = -S_1^x S_2^x - S_1^y S_2^y + S_1^z S_2^z$ , the ground state and first excited state have parities equal to 1 and  $-1$ , respectively. (This can be proved using the Perron-Frobenius theorem for a real symmetric matrix.) We now consider the entire system with  $2N$  sites. In the limit  $\kappa \rightarrow 0$ , the ground state of the system is given by a direct product of ground states over the bonds  $(1, 2), (3, 4), \dots, (2N-1, 2N)$ . Since there are  $N$  dimers, the parity of this state is  $(-1)^{2SN}$ , while the parity of the first excited state is  $(-1)^{2SN+1}$ . On the other hand, in the limit  $\kappa \rightarrow \infty$ , the ground state of the system is given by a direct product of ground states over the bonds  $(2, 3), (4, 5), \dots, (2N, 1)$ . Under parity, the parity of this state is  $(-1)^{2SN+2S}$ , while the parity of the first excited state is  $(-1)^{2SN+2S+1}$ . A comparison between the ground states in the two limits shows that they have a relative parity of  $(-1)^{2S}$ .

### III. TUNNELING APPROACH TO THE FINITE SPIN CHAIN

In this section, we will study the model defined in Eq. (6) using a tunneling approach. We are interested in the limit  $S \rightarrow \infty$  and  $\kappa \rightarrow 0$ , such that  $\kappa S$  is of order 1. We will compute

the action of the system and use that to compute the tunneling amplitude between the two Néel states.

In the limit  $\kappa \rightarrow 0$ , the system consists of decoupled dimers whose energy levels are easy to compute. We will assume in this section that there are at least three dimers, i.e.,  $N \geq 3$ . For the dimer on the bond  $(2n-1, 2n)$ , we define the variables

$$\vec{\phi}_n = \frac{\vec{S}_{2n-1} - \vec{S}_{2n}}{2S},$$

$$\vec{l}_n = \vec{S}_{2n-1} + \vec{S}_{2n}. \quad (8)$$

These variables satisfy the relations

$$\vec{\phi}_n^2 = 1 + \frac{1}{S} - \frac{\vec{l}_n^2}{4S^2},$$

$$\vec{\phi}_n \cdot \vec{l}_n = 0,$$

$$[J_m^a, \phi_n^b] = i \delta_{mn} \sum_c \epsilon^{abc} \phi_n^c,$$

$$[J_m^a, l_n^b] = i \delta_{mn} \sum_c \epsilon^{abc} l_n^c,$$

$$[\phi_m^a, \phi_n^b] = \frac{i}{4S^2} \delta_{mn} \sum_c \epsilon^{abc} l_n^c. \quad (9)$$

Several simplifications occur in the classical limit  $S \rightarrow \infty$ . First, in the Néel state,  $\vec{l}$  is equal to zero while  $\vec{\phi}$  is a unit vector; the latter is clear from the first equation in Eq. (9). We will therefore set  $\vec{\phi}_n^2 = 1$  exactly. Second, we will take the commutator  $[\phi_m^a, \phi_n^b] = 0$  due to the fourth equation in Eq. (9). Finally, given the second and third equations in Eq. (9), we can obtain the momentum which is canonically conjugate to  $\phi_n$ , namely,  $\vec{l}_n = \vec{\phi}_n \times \vec{\Pi}_n$ , which satisfies the commutation relation

$$[\phi_m^a, \Pi_n^b] = i \delta_{mn} \delta_{ab}. \quad (10)$$

Using Eq. (8), we can write the Hamiltonian in Eq. (6) in terms of  $\vec{\phi}$  and  $\vec{\Pi}$ , and then obtain the Lagrangian as

$$L = \sum_{n=1}^N \frac{d\vec{\phi}_n}{dt} \cdot \vec{\Pi}_n - H. \quad (11)$$

We eventually find that

$$L = \sum_{n=1}^N \frac{1}{2} \left( \frac{d\vec{\phi}_n}{dt} \right)^2 + \kappa S^2 \sum_{n=1}^{N-1} \vec{\phi}_n \cdot \vec{\phi}_{n+1}$$

$$+ \kappa S^2 [-\phi_N^x \phi_1^x - \phi_N^y \phi_1^y + \phi_N^z \phi_1^z]$$

$$+ \frac{\kappa S}{2} \sum_{n=1}^{N-1} \left( \frac{d\vec{\phi}_n}{dt} + \frac{d\vec{\phi}_{n+1}}{dt} \right) \cdot \vec{\phi}_n \times \vec{\phi}_{n+1}$$

$$+ \frac{\kappa S}{2} \left[ \left( \frac{d\phi_N^x}{dt} - \frac{d\phi_1^x}{dt} \right) (\phi_N^y \phi_1^z + \phi_N^z \phi_1^y) \right]$$

$$\begin{aligned}
& + \left( \frac{d\phi_N^y}{dt} - \frac{d\phi_1^y}{dt} \right) (-\phi_N^z \phi_1^x - \phi_N^x \phi_1^z) \\
& + \left( \frac{d\phi_N^z}{dt} + \frac{d\phi_1^z}{dt} \right) (-\phi_N^x \phi_1^y + \phi_N^y \phi_1^x) \Big] \\
& + \kappa^2 S^2 [\text{terms of fourth order in } \vec{\phi}_n]. \quad (12)
\end{aligned}$$

The terms in the third line of this Lagrangian are what give rise to the topological term in Eq. (4) in the continuum limit. In the last line of Eq. (12), the terms of fourth order in  $\vec{\phi}_n$  are chosen in such a way that when we compute the Hamiltonian from it, it agrees with Eq. (6). We will now see why these fourth order terms are not important.

In the limit  $\kappa \rightarrow 0$ ,  $S \rightarrow \infty$ , and  $\kappa S$  of order 1, we can scale the time  $t$  by a factor of  $\sqrt{S}$  to show that only the first two lines of Eq. (12) contribute to the Euler-Lagrange equations of motion (EOM); this is a major simplification. To compute the tunneling amplitude between the two Néel states, we will find the solutions of the EOM in imaginary time. We then find that the tunneling amplitude comes with a phase which arises from the third through sixth lines of Eq. (12); thus these terms are important even though they do not directly contribute to the EOM. The fourth order terms in the last line of Eq. (12) do not contribute to either the EOM or the phase, and we will therefore ignore them henceforth.

In imaginary time (denoted by the symbol  $\tau$ ), the action takes the form

$$\begin{aligned}
S_I = & \int d\tau \left[ \sum_{n=1}^N \frac{1}{2} \left( \frac{d\vec{\phi}_n}{d\tau} \right)^2 + \kappa S^2 \left( N - \sum_{n=1}^{N-1} \vec{\phi}_n \cdot \vec{\phi}_{n+1} \right) \right. \\
& + \kappa S^2 [\phi_N^x \phi_1^x + \phi_N^y \phi_1^y - \phi_N^z \phi_1^z] \\
& - i \frac{\kappa S}{2} \sum_{n=1}^{N-1} \left( \frac{d\vec{\phi}_n}{d\tau} + \frac{d\vec{\phi}_{n+1}}{d\tau} \right) \cdot \vec{\phi}_n \times \vec{\phi}_{n+1} \\
& - i \frac{\kappa S}{2} \left[ \left( \frac{d\phi_N^x}{d\tau} - \frac{d\phi_1^x}{d\tau} \right) (\phi_N^y \phi_1^z + \phi_N^z \phi_1^y) \right. \\
& + \left( \frac{d\phi_N^y}{d\tau} - \frac{d\phi_1^y}{d\tau} \right) (-\phi_N^z \phi_1^x - \phi_N^x \phi_1^z) \\
& \left. + \left( \frac{d\phi_N^z}{d\tau} + \frac{d\phi_1^z}{d\tau} \right) (-\phi_N^x \phi_1^y + \phi_N^y \phi_1^x) \right] \Big]. \quad (13)
\end{aligned}$$

We have introduced a constant  $\kappa S^2 N$  in Eq. (13) so that the action vanishes for each of the two Néel states. The tunneling amplitude will be given by the sum of  $\exp(-S_I)$  along all the paths of extremal action which join the Néel states. We will now determine these extremal paths.

Let us use polar angles to write the variables  $\vec{\phi}_n = (\sin \alpha_n \cos \beta_n, \sin \alpha_n \sin \beta_n, \cos \alpha_n)$ . The Néel states 1 and 2 are given by  $\alpha_n = 0$  for all  $n$  and  $\alpha_n = \pi$  for all  $n$ , respectively. We now solve the EOM following from the first two lines of Eq. (13) in order to obtain the paths going from state 1 to state 2. We will not write the EOM explicitly here, but directly present the solutions. We find that the two paths which have the least action are given by

- (a)  $\alpha_n(\tau) = \alpha(\tau)$  and  $\beta_n = \beta_0 + (n\pi/N)$  for all  $n$ , and
- (b)  $\alpha_n(\tau) = \alpha(\tau)$  and  $\beta_n = \beta_0 - (n\pi/N)$  for all  $n$ ,

where  $\beta_0$  is an arbitrary angle. In both cases, the function  $\alpha(\tau)$  satisfies the EOM

$$\frac{d^2 \alpha}{d\tau^2} = \kappa S^2 \sin(2\alpha) \left( 1 - \cos \frac{\pi}{N} \right), \quad (14)$$

with the boundary conditions  $\alpha(-\infty) = 0$ ,  $\alpha(\infty) = \pi$ , and  $d\alpha(\pm\infty)/d\tau = 0$ . This implies that

$$\frac{d\alpha}{d\tau} = 2S\sqrt{\kappa} \sin \alpha \sin \frac{\pi}{2N}. \quad (15)$$

Using this we can evaluate the contribution of the first two lines of Eq. (13) along either one of the paths joining the Néel states. We find that the real part of the action is given by

$$\begin{aligned}
\text{Re } S_I = & N \int_{-\infty}^{\infty} d\tau \left[ \frac{1}{2} \left( \frac{d\alpha}{d\tau} \right)^2 + \kappa S^2 \sin^2 \alpha \left( 1 - \cos \frac{\pi}{N} \right) \right] \\
= & 4\sqrt{\kappa} SN \sin \frac{\pi}{2N}. \quad (16)
\end{aligned}$$

We can now evaluate the contribution of the imaginary terms in Eq. (13) to the action. We find that for path (a), they contribute  $-i2\kappa SN \sin(\pi/N)$ , while for path (b), they contribute  $i2\kappa SN \sin(\pi/N)$ . Hence the total contribution of the two paths to  $\exp(-S_I)$  is given by

$$\Delta \sim \cos \left( 2\kappa SN \sin \frac{\pi}{N} \right) \exp \left( -4\sqrt{\kappa} SN \sin \frac{\pi}{2N} \right), \quad (17)$$

up to some prefactors which are determined by fluctuations about the classical paths. Since  $\Delta$  is the matrix element between two classically degenerate states, the energy gap between the two states is given by  $2|\Delta|$ . We thus see that the gap vanishes if  $2\kappa SN \sin(\pi/N)$  is an odd multiple of  $\pi/2$ , i.e., if

$$4\kappa SN \sin \frac{\pi}{N} = \pi \text{ modulo } 2\pi. \quad (18)$$

This is the same condition as the one satisfied by the parameter  $\theta$  in Sec. II A in the limits  $S, N \rightarrow \infty$  and  $\kappa \rightarrow 0$ . Further, if  $4\kappa SN \sin(\pi/N) = 0 \text{ modulo } 2\pi$ , the gap is given by  $\exp(-\text{Re } S_I)$  which agrees with the expression  $\exp(-2\pi/g)$  given in Sec. II A for  $S, N \rightarrow \infty$  and  $\kappa \rightarrow 0$ . Thus a simple quantum mechanical tunneling calculation seems to reproduce the same conditions as those obtained earlier by more complex field theoretic calculations involving topological terms and a renormalization group analysis.

Before ending this section, we should note that there are other pairs of paths with extremal action, which have the form

- (a)  $\alpha_n(\tau) = \alpha(\tau)$  and  $\beta_n = \beta_0 + (pn\pi/N)$  for all  $n$ , and
- (b)  $\alpha_n(\tau) = \alpha(\tau)$  and  $\beta_n = \beta_0 - (pn\pi/N)$  for all  $n$ ,

where  $p=3, 5, \dots$  (going up to the largest odd integer  $\leq N-1$ ) labels the different pairs of paths. However, the real part of the action of these paths is given by  $4\sqrt{\kappa} SN \sin(p\pi/2N)$ , which, for large  $S$ , is much larger than

the expression given in Eq. (16); their contributions to the tunneling amplitude are therefore much smaller.

Finally, we would like to note that it is important that the twist in the boundary condition should be by  $\pi$ , and not by any other angle. Even though any nonzero twist would lead to two Néel ground states classically, the pairs of tunneling paths between those two ground states would not have the same real part of the action if the twist angle was different from  $\pi$ . The pairs of paths would therefore not cancel each other no matter what the imaginary parts of their actions are. This is because two complex numbers cannot add up to zero, no matter what their phases are, if their magnitudes are not equal.

#### IV. A SECOND APPROACH TO THE MATRIX ELEMENT BETWEEN NÉEL STATES

In the previous section we argued that the gapless points of the Hamiltonian in Eq. (6) can be identified with the values of  $\kappa$  for which the tunneling amplitude between the two classical ground states vanish. In this section we will calculate this amplitude using an alternate method.

The twist on the edge bond  $(2N, 1)$  breaks the global  $SU(2)$  symmetry and thus lifts the continuous degeneracy of the classical ground states. With the twist, the two degenerate ground states of the Hamiltonian are the Néel states which are connected to each other by rotation by  $\pi$  about the  $y$  axis,

$$|N_1\rangle = |S, -S, S, \dots, -S, S, -S\rangle,$$

and

$$|N_2\rangle = |-S, S, -S, \dots, S, -S, S\rangle, \quad (19)$$

where  $|\{m_i\}\rangle$  denotes the state with  $S_i^z$  eigenvalue  $m_i$ .

We are interested in the zeroes of the quantity

$$T = \langle N_2 | e^{-\beta H} | N_1 \rangle, \quad (20)$$

as a function of  $\kappa$ , and  $\beta = 1/k_B T$  can be thought of as either the inverse temperature or imaginary time. Though the calculation of the above matrix element is an interacting many-body problem, we can obtain its zeroes “exactly” in the thermodynamic limit.

First we note that, in the expansion of the exponential,

$$e^{-\beta H} = \sum_{n=0}^{\infty} \frac{(-\beta H)^n}{n!}, \quad (21)$$

the first term which makes a nonzero contribution to  $T$  has  $n = 2SN$ . This is because to take  $|N_1\rangle$  to  $|N_2\rangle$ , spins belonging to the  $A$ -sublattice have to be flipped from  $|S\rangle$  to  $|-S\rangle$ , and this requires the action of  $(S^-)^{2S}$  for each spin. Similarly, the action of  $(S^+)^{2S}$  will take spins in the  $B$ -sublattice from  $|-S\rangle$  to  $|S\rangle$ .

Next, we will calculate the values of  $\kappa$  for which

$$\langle N_2 | H^{2SN} | N_1 \rangle = 0. \quad (22)$$

Then we will show that as  $N \rightarrow \infty$ , Eq. (22) implies that

$$\langle N_2 | H^{2SN+k} | N_1 \rangle = 0 \quad (23)$$

for any finite  $k$ . This in turn will imply that  $T$  is zero.

The only term in  $H^{2SN}$  which makes a nonzero contribution to the left-hand side of Eq. (22) is

$$\prod_{i=1}^N (S_{2i}^-)^{2S} (S_{2i+1}^+)^{2S}.$$

We need to count the number of ways in which such a term can arise. The contribution comes from terms of the following type:

$$\prod_{i=1}^N (S_{2i}^- S_{2i+1}^+)^m (S_{2i-1}^+ S_{2i}^-)^{2S-m}, \quad (24)$$

where  $0 \leq m \leq 2S$ . The above term can be obtained in

$$\frac{(2SN)!}{(m!)^N [(2S-m)!]^N}$$

ways and comes with a weight  $(-1)^m \kappa^{mN}$ . Here we have neglected an overall  $m$ -independent factor due to the Clebsch-Gordon coefficients arising from the repeated application of  $S^+$  and  $S^-$  operators. The condition in Eq. (22) then becomes

$$\sum_{m=0}^{2S} (-1)^m (a_m(\kappa))^N = 0, \quad (25)$$

where

$$a_m(\kappa) = \frac{\kappa^m}{m!(2S-m)!}.$$

Before proceeding further, we note that the above condition preserves the duality symmetry under  $\kappa \rightarrow 1/\kappa$ . This is because Eq. (25) can be written as

$$\kappa^{2SN} (-1)^{2S} \sum_m (-1)^m (a_m(1/\kappa))^N = 0. \quad (26)$$

Hence if  $\kappa^*$  is a solution, so is  $1/\kappa^*$ . Thus we can restrict ourselves to the range  $0 \leq \kappa \leq 1$ .

Equation (25) determines the roots of a polynomial of order  $2SN$ , which, in general, cannot be solved analytically. But it turns out that we can obtain the roots in the limit  $N \rightarrow \infty$ . In this limit, depending on the value of  $\kappa$ , one particular term in the sum is predominant, and the rest of the terms can be neglected compared to this. The dominant term is determined by

$$\max_m a_m \equiv a_{m^*}. \quad (27)$$

As  $\kappa$  varies from 0 to 1,  $m^*$  successively takes values  $m^* = 0, 1, \dots, S$  for integer  $S$  and  $m^* = 0, 1, \dots, S + 1/2$  for half-odd-integer  $S$ . Noting that neighboring terms in the sum have opposite signs, Eq. (25) can be satisfied only when

$$a_m = a_{m+1}. \quad (28)$$

Thus the gapless points are given by

$$\kappa_m^* = \frac{m+1}{2S-m}, \quad (29)$$

where  $m=0, 1, \dots, S-1$  for integer  $S$  and  $m=0, 1, \dots, S-1/2$  for half-odd-integer  $S$ .

To complete our argument that Eq. (29) gives the gapless points, we need to show that Eq. (22) implies Eq. (23). To this end, we first note that the nonzero contributions to the matrix element from  $H^{2SN+k}$  can be obtained from the contributing terms in  $H^{2SN}$ , given in Eq. (24), by adding terms of the form  $S_i^z S_{i+1}^z$ ,  $S_i^+ S_{i+1}^-$ , or  $S_i^- S_{i+1}^+$ . Now the weight coming from the Clebsch-Gordon coefficients depends on the order in which the terms appear. But formally one can write that Eq. (23) implies

$$\sum_m (-1)^m b_{m,k} (a_m(\kappa))^N = 0, \quad (30)$$

where  $b_{m,k}$  are finite undetermined constants independent of  $N$ . As before, in the large- $N$  limit, the left-hand side of Eq. (30) can be zero only through the mutual cancellation of a pair of neighboring terms, i.e., when

$$\frac{a_m}{a_{m+1}} = \left( \frac{b_{m+1}}{b_m} \right)^{1/N}. \quad (31)$$

As  $N \rightarrow \infty$ , this reduces to the condition in Eq. (28). In other words, the vanishing of  $\langle N_2 | H^{2SN} | N_1 \rangle$  is a sufficient condition for the vanishing of  $\langle N_2 | H^{2SN+k} | N_1 \rangle$  for any finite  $k$  as  $N \rightarrow \infty$ .

For half-odd-integer spins,  $\kappa^* = 1$  is a solution of Eq. (29) for  $m=S-1/2$ , but it is *not* a solution for integer spins. This is consistent with Haldane's conjecture<sup>1</sup> that the uniform chain is gapless for half-odd-integer spins and gapped for integer spins.

Since the identification of gapless points with the zeroes of the transition amplitudes between the two Néel states is essentially a semiclassical approximation, we expect the formula given by Eq. (29) to get better for larger values of  $S$ .

As with the tunneling calculation in Sec III, here also one can see that it is crucial to have a twist by  $\pi$  and not any other angle. Let us suppose that the twist angle is  $\chi$ . Then the Hamiltonian for the bond between the spins at sites  $2N$  and  $1$  will be

$$\kappa(S_{2N}^z S_1^z + e^{i\chi} S_{2N}^+ S_1^- + e^{-i\chi} S_{2N}^- S_1^+).$$

Then the equivalent of the condition in Eq. (28) will read

$$a_m = -e^{i\chi} a_{m+1}. \quad (32)$$

Since  $a_m$ 's are all real and positive, such a condition can be satisfied only when  $\chi = \pi$ , in which case Eq. (32) becomes Eq. (28).

Finally, let us compare the gapless values of  $\kappa$  given in Eq. (29) with those given in Eq. (18) in the limit  $N \rightarrow \infty$ , namely,

$$\kappa_m^* = \frac{m+1/2}{2S}, \quad (33)$$

where  $m=0, 1, \dots$ . Since Eq. (18) was derived under the assumption that  $S \rightarrow \infty$  and  $\kappa S$  is of order 1, we must restrict  $m$

to be much less than  $S$  in Eq. (33). We see that for large values of  $S$  and  $m \ll S$ , the values of  $\kappa_m^*$  in Eqs. (29) and (33) are related by a shift of  $1/(4S)$ . It would be useful to understand more deeply why this is so. Heuristically, this discrepancy can be explained by postulating that the phase difference between the actions for the two paths discussed in Sec. III has an additional factor of  $\pi$  for some reason. Equation (18) would then change to  $4\pi\kappa S = 0$  modulo  $2\pi$  for  $N \rightarrow \infty$ ; this condition would be equivalent to Eq. (29) for  $m \ll S$ . In a different problem (tunneling of a charged particle in two dimensions in the presence of a large magnetic field), it was empirically found that an additional factor of  $\pi$  appears due to fluctuations about the tunneling paths.<sup>20</sup> It may be worth studying if something similar happens in our problem.

## V. NUMERICAL RESULTS FOR FINITE SYSTEMS

In this section, we numerically determine the values of  $\kappa$  for which the Hamiltonian becomes gapless using exact diagonalization of finite systems with  $2N$  sites. These results, being a direct calculation of the gapless points, will give us information about the physical regimes in which the analytical methods outlined in Secs. III and IV are valid.

We begin with a brief outline of the method used to find the gapless points. As we vary  $\kappa$  in Eq. (1), it is known that the gapless points separate various phases whose ground states are represented approximately by different valence bond states (see Refs. 12 and 21 and references therein). Specifically, for a given spin  $S$ , there are  $2S+1$  different phases separated by the  $2S$  gapless points for  $\kappa$  between 0 and  $\infty$ . The lowest two eigenstates of an untwisted Hamiltonian never cross each other in energy, even at the transition from one phase to the other; also, the ground state always has the same eigenvalue  $(-1)^{2SN}$  for the parity  $P$ . It is here that we make use of the twisted boundary condition in Eq. (6). It has been shown<sup>12</sup> that the lowest two eigenstates of this Hamiltonian (both of which lie in the  $S_{\text{tot}}^z = 0$  sector) have different parity eigenvalues, and they cross at certain points which, in the limit  $N \rightarrow \infty$ , become the gapless points of the Hamiltonian in Eq. (1). This means that one can locate the gapless points of the Hamiltonian in Eq. (1) by studying the crossing of the two lowest eigenvalues of the Hamiltonian in Eq. (6) in *different parity sectors*. This enables us to find the gapless points without having to consider two very closely spaced eigenvalues lying within a single symmetry sector.

We study the Hamiltonian in Eq. (6) numerically. Because of the duality between  $\kappa$  and  $1/\kappa$  we restrict our studies to  $0 \leq \kappa \leq 1$ . We use the Lanczos algorithm to diagonalize finite systems from  $N=3$  to 5. Spins from  $S=2$  to 3 are studied for  $N=3$  to 5, but for  $S=3.5$  to 7 we restrict ourselves to  $N=3$  and 4 due to computational limitations.

In Fig. 1, we present two representative data plots, for  $N=3$ . The upper plot is for  $S=3.5$  and the lower one is for  $S=4$ . Plotted on the  $y$  axis in both figures is  $E(P=-1) - E(P=+1)$ , the energy difference between the two lowest energy eigenstates in the two parity sectors. Wherever the plot crosses the  $x$  axis we have a gapless point of the Hamiltonian in Eq. (1). The values of the crossing points are indicated in the plots. From the discussion in Sec. II, we know

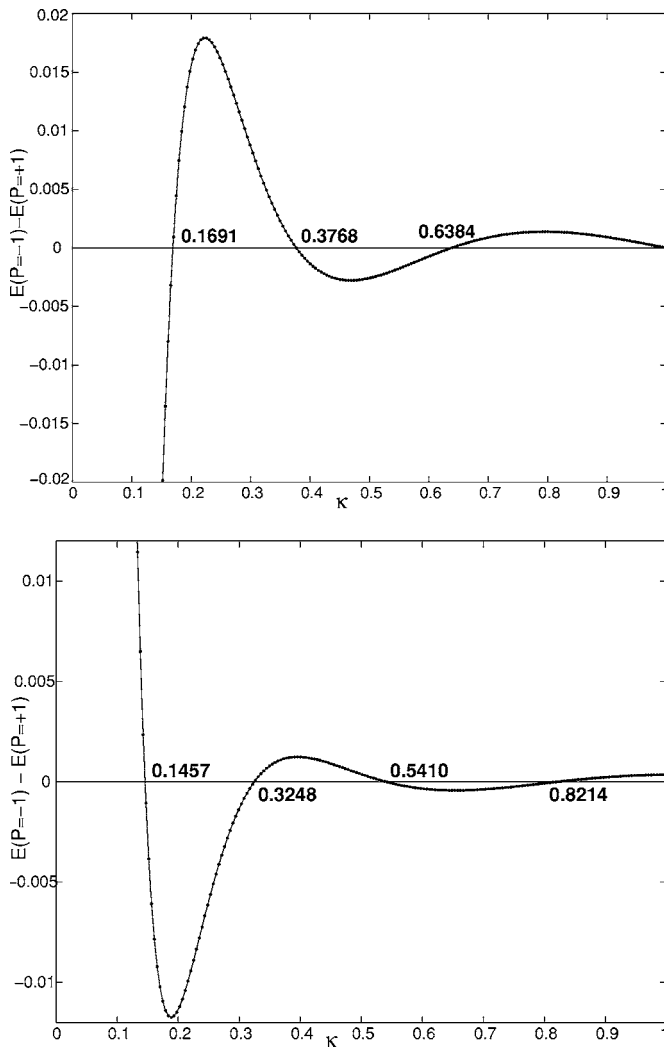


FIG. 1. Energy difference between the two lowest energies in the  $P=-1$  and  $P=+1$  sectors as a function of  $\kappa$ , for  $N=3$ . The upper figure is for  $S=3.5$ , and the lower figure is for  $S=4$ . The locations of the gapless points are shown.

that the ground state for  $N=3$ ,  $S=3.5$  should have a parity  $-1$ , and for  $N=3$ ,  $S=4$  should have a parity  $+1$ . This is indeed borne out by the plots in the figure. Moreover, the gapless point at  $\kappa=1$  is also present for  $S=3.5$  as expected. The nature of these plots for other spins and different lattice sizes is similar. Since our emphasis in this work is on the locations of the gapless points, we now turn to analyzing those points more closely. [Incidentally, we observe in Fig. 1 that the envelope of the magnitude of the gap is rapidly decreasing with increasing  $\kappa$ ; this is in accordance with the exponential factor for the tunneling amplitude in Eq. (17).]

Figure 2 shows a comparison of the different methods used to calculate the gapless points. Plotted on the y axis is  $\kappa^1$ , the gapless point closest to the origin for various values of the spin, for  $N=3$ . The topmost plot (marked by dots) is for values obtained from the numerical calculations, called  $\kappa_{num}^1$ . The next plot (crosses) is for values obtained from the Néel state calculation in Eq. (25),  $\kappa_{Neel}^1$ . The plot at the bottom (squares) is for values obtained from the tunneling expression in Eq. (18),  $\kappa_{tum}^1$ . Clearly, the values of  $\kappa^1$  obtained

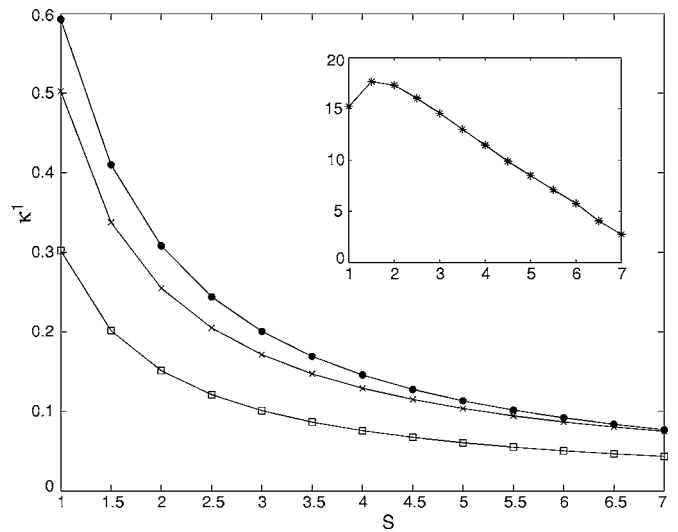


FIG. 2. The location  $\kappa^1$  of the gapless point closest to zero, as a function of the spin, for  $N=3$ . The results from numerical calculations (dots), Néel state calculations (crosses), and tunneling calculations (squares) are shown. The joining lines are guides for the eye. The inset shows the percentage variation of the Néel state calculations when compared with the numerical results.

using the Néel state calculation are in closer agreement with the numerical values than the tunneling values. The tunneling values do not converge with increasing  $S$ , even though one is looking at data for spin values as large as  $S=7$ . On the other hand, the plot of values using the Néel state calculations converges much faster. This is made clearer in the plot by the inset where on the y axis we have plotted the percentage deviation,  $[(\kappa_{num}^1 - \kappa_{Neel}^1) / \kappa_{num}^1] \times 100$ , of the values of  $\kappa_{Neel}^1$  from the numerically obtained values.

Figure 3 shows a comparison between the numerical results (dots) and those obtained from the Néel state calculation (crosses) for  $\kappa^*$ , the gapless point closest to  $\kappa=1$ . (Unlike in Fig. 2, we have not shown the tunneling results based on Eq. (18) because that formula for the gapless points is not valid when  $\kappa$  is close to 1.) The data sets for integer and half-odd-integer spins have been plotted separately. The plot and the inset at the top are for integer spins, and the ones at the bottom are for half-odd-integer spins. As before, we see that the agreement with the numerical results improves as we go to larger spins. We also see from the insets that for a given spin, the agreement is much better near  $\kappa=1$  than it was near  $\kappa=0$ . This suggests that the Néel state calculation gets better as we increase  $\kappa$  from 0 to 1. This is something which is seen very clearly in Table I. (For the cases  $S=1$  and  $1.5$ , there is only one gapless point for  $\kappa < 1$ . Hence the same values of  $\kappa$  appear in Figs. 2 and 3 for those two cases.)

Table I shows how the numerical results, the Néel state calculations [Eq. (25)], and the tunneling results [Eq. (18)] compare for the gapless points. The table shows the values of  $\kappa$  at which the Hamiltonian in Eq. (6) is gapless for  $S=6.5$  (top half) and  $S=7$  (bottom half), for  $N=3$ . The percentage deviations as defined earlier are also shown for the Néel state and tunneling calculations. As conjectured after looking at Fig. 3, we see that the Néel state calculation gives successively better approximations to the actual gapless points as

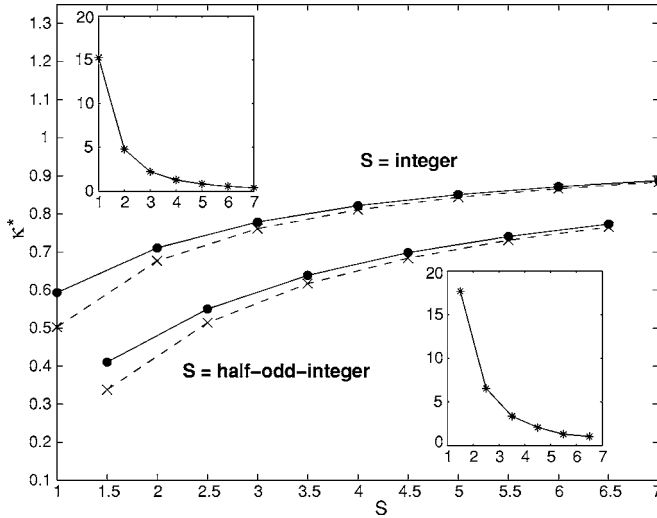


FIG. 3. The location  $\kappa^*$  of the gapless point closest to (but less than) 1, as a function of the spin, for  $N=3$ . The results from numerical calculations (dots) and Néel state calculations (crosses) are shown. The top and bottom parts of the figure are for integer and half-odd-integer values of the spin, respectively. The joining lines are guides for the eye. The insets show the percentage variation of the Néel state calculations when compared with the numerical results.

we go further from the origin  $\kappa=0$ . We have shown the tunneling values for all the gapless points only for completion; the formula given by Eq. (18) is valid only for  $\kappa S$  of order 1. We again see that these values have much larger percentage deviations from the values obtained from the other two methods, even though the values of the spins considered are quite large.

We now look at how the values of  $\kappa$  at the gapless points change with  $N$  and see how the  $N \rightarrow \infty$  values compare with

TABLE I. Comparison of the values of all the gapless points obtained using the three methods of calculating them [ $\kappa_{num}$  from numerical results,  $\kappa_{Neel}$  from Eq. (25), and  $\kappa_{tun}$  from Eq. (18)], for  $S=6.5$  (top half) and 7 (bottom half). The data presented is for  $N=3$ .

$\kappa_{num}$	$\kappa_{Neel}$	% deviation	$\kappa_{tun}$	% deviation
0.083	0.080	3.6	0.047	45.4
0.190	0.180	5.2	0.140	26.3
0.306	0.293	4.2	0.232	24.2
0.438	0.424	3.2	0.326	25.6
0.773	0.765	1.0	0.512	33.8
1	1	0		
0.077	0.074	3.9	0.043	44.2
0.174	0.166	4.0	0.130	25.3
0.281	0.269	5.0	0.252	23.1
0.400	0.387	3.3	0.302	24.5
0.536	0.525	2.1	0.389	27.4
0.695	0.685	1.3	0.475	31.7
0.887	0.884	0.3	0.561	36.8

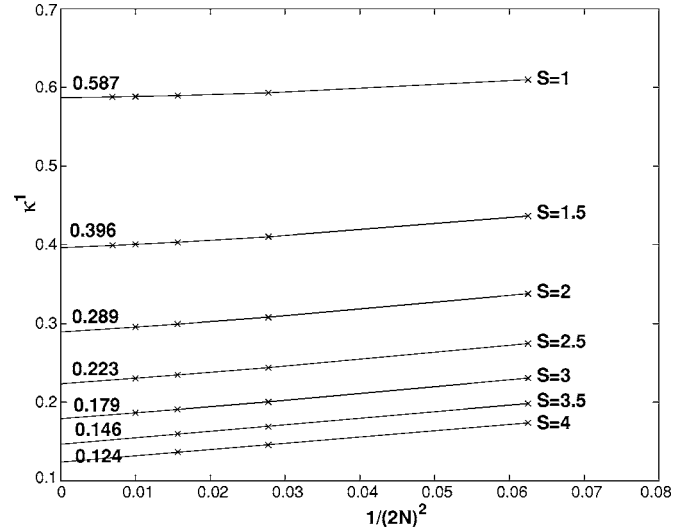


FIG. 4. Variation of  $\kappa^1$  with  $N$  for values of  $S$  from 1 to 4. The numbers at the left of each graph are the  $N \rightarrow \infty$  extrapolated values. The crosses indicate values of  $\kappa^1$  obtained numerically.

those given by Eq. (29). We take  $\kappa^1$  as an example. Figure 4 shows the behavior for  $S$  going from 1 to 4. The crosses indicate values of  $\kappa^1$  obtained numerically for various values of  $S$  and  $N$ ;  $N$  goes from 2 to 6 for  $S=1$  and 1.5, from 2 to 5 for  $S=2$  to 3, and from 2 to 4 for  $S=3.5$  and 4. We find the  $N \rightarrow \infty$  values by extrapolating the best fits obtained by fitting the data to even polynomials in  $1/(2N)^2$  following Ref. 13.

The extrapolated values of  $\kappa^1$  in the  $N \rightarrow \infty$  limit and the corresponding values obtained from Eq. (29) (in parentheses) for  $S=1, 1.5, 2, 2.5, 3.0, 3.5,$  and  $4.0$  are given by 0.587 (0.500), 0.396 (0.333), 0.289 (0.250), 0.223 (0.200), 0.179 (0.167), 0.146 (0.143), and 0.124 (0.125) respectively. Clearly, the agreement between the two sets of values gets better for larger values of the spin. The extrapolated values of  $\kappa^1$  for  $S=1, 1.5,$  and  $2$  agree well with the values of 0.588, 0.397, and 0.290 obtained previously by the quantum Monte Carlo method.<sup>13</sup>

## VI. CONCLUSIONS

We have used three different techniques to find the gapless points of a dimerized spin- $S$  chain with a finite number of sites and with a twisted boundary condition. The first technique uses a tunneling approach which is expected to be valid in the limit  $S \rightarrow \infty$ ,  $\kappa \rightarrow 0$ , and  $\kappa S$  of order 1. Remarkably, we find that a quantum mechanical tunneling calculation reproduces the same expressions for the locations of the gapless points and the gap as those obtained by more involved field theoretic techniques.

However, a direct numerical study of the gapless points shows a systematic deviation from the tunneling results in the limit discussed above. It would be useful to know why the tunneling results differ systematically from the numerical results in this limit. One possible idea is to examine if an additional factor of  $\pi$  appears in the fluctuation prefactor of the tunneling amplitude as mentioned at the end of Sec. IV.

In view of the discrepancy between the tunneling and numerical results, we have presented a second analytical derivation of the gapless points which is based on a calculation of the matrix element between the two Néel states to lowest order in powers of the Hamiltonian; this derivation is expected to become more accurate as the number of sites becomes large. We find that the results obtained by this approach agree much better with the numerical results than the tunneling results, even in the limit  $\kappa \rightarrow 0$ . It may be instructive to understand in more detail why there is such a good agreement between this relatively simple analytical calculation and the numerical results.

One of the features of the numerical results shown above is that the Néel state calculation always underestimates the

values of  $\kappa$  which correspond to gapless points, while all the time getting closer to the actual values with increasing  $S$  (given  $N$ ) or increasing  $N$  (given  $S$ ). This may indicate positive corrections of order  $1/N$  and  $1/S$  to the formula obtained from the Néel state calculation.

#### ACKNOWLEDGMENTS

V.R.C. thanks CSIR, India for financial support. We thank DST, India for financial support under the project SP/S2/M-11/2000.

- 
- <sup>1</sup>F. D. M. Haldane, Phys. Lett. **93A**, 464 (1983); Phys. Rev. Lett. **50**, 1153 (1983).  
<sup>2</sup>W. J. L. Buyers, R. M. Morra, R. L. Armstrong, M. J. Hogan, P. Gerlach, and K. Hirakawa, Phys. Rev. Lett. **56**, 371 (1986); J. P. Renard, M. Verdaguer, L. P. Regnault, W. A. C. Erkelens, J. Rossat-Mignod, and W. G. Stirling, Europhys. Lett. **3**, 945 (1987); S. Ma, C. Broholm, D. H. Reich, B. J. Sternlieb, and R. W. Erwin, Phys. Rev. Lett. **69**, 3571 (1992).  
<sup>3</sup>I. Affleck, in *Fields, Strings and Critical Phenomena*, edited by E. Brezin and J. Zinn-Justin (North-Holland, Amsterdam, 1989).  
<sup>4</sup>E. Fradkin, *Field Theories of Condensed Matter Systems* (Addison-Wesley, Reading, MA, 1991).  
<sup>5</sup>A. Auerbach, *Interacting Electrons and Quantum Magnetism* (Springer-Verlag, New York, 1994).  
<sup>6</sup>G. Sierra, in *Strongly Correlated Magnetic and Superconducting Systems*, edited by G. Sierra and M. A. Martin-Delgado, Lecture Notes in Physics Vol. 478 (Springer, Berlin, 1997).  
<sup>7</sup>A. M. M. Pruisken, R. Shankar, and N. Surendran, Phys. Rev. B **72**, 035329 (2005).  
<sup>8</sup>R. R. P. Singh and M. P. Gelfand, Phys. Rev. Lett. **61**, 2133 (1988).  
<sup>9</sup>Y. Kato and A. Tanaka, J. Phys. Soc. Jpn. **63**, 1277 (1994).  
<sup>10</sup>S. Pati, R. Chitra, D. Sen, H. R. Krishnamurthy, and S. Ramasesha, Europhys. Lett. **33**, 707 (1996).  
<sup>11</sup>K. Totsuka, Y. Nishiyama, N. Hatano, and M. Suzuki, J. Phys.: Condens. Matter **7**, 4895 (1995).  
<sup>12</sup>A. Kitazawa and K. Nomura, J. Phys. Soc. Jpn. **66**, 3379 (1997).  
<sup>13</sup>M. Nakamura and S. Todo, Phys. Rev. Lett. **89**, 077204 (2002).  
<sup>14</sup>R. Shankar and N. Read, Nucl. Phys. B **336**, 457 (1990); I. Affleck, Phys. Rev. Lett. **56**, 408 (1986).  
<sup>15</sup>A. Kitazawa, J. Phys. A **30**, L285 (1997).  
<sup>16</sup>I. Affleck, D. Gepner, H. J. Schulz, and T. Ziman, J. Phys. A **22**, 511 (1989).  
<sup>17</sup>K. Okamoto and K. Nomura, Phys. Lett. A **169**, 433 (1992).  
<sup>18</sup>K. Nomura, J. Phys. A **28**, 5451 (1995).  
<sup>19</sup>M. Kolb, Phys. Rev. B **31**, 7494 (1985).  
<sup>20</sup>J. K. Jain and S. Kivelson, Phys. Rev. B **37**, 4111 (1988).  
<sup>21</sup>M. Oshikawa, J. Phys.: Condens. Matter **4**, 7469 (1992).